Veterinary Microbiology 238 (2019) 108436

Contents lists available at ScienceDirect

Veterinary Microbiology

journal homepage: www.elsevier.com/locate/vetmic

U18666A inhibits classical swine fever virus replication through interference with intracellular cholesterol trafficking

Xiao-Dong Liang, Yun-Na Zhang, Chun-Chun Liu, Jing Chen, Xiong-Nan Chen, Abdul Sattar Baloch, Bin Zhou*

MOE Joint International Research Laboratory of Animal Health and Food Safety, College of Veterinary Medicine, Nanjing Agricultural University, Nanjing, China

ARTICLE INFO

Keywords:
Classical swine fever virus (CSFV)
Cholesterol
U18666A
Antiviral activity
NPC1

ABSTRACT

The level of cholesterol in host cells has been demonstrated to affect viral infection. Our previous studies showed that cholesterol-rich membrane rafts mediated the entry of classical swine fever virus (CSFV) into PK-15 or 3D4/21 cells, but the role of cholesterol post entry was still not clear. In this study, we found that CSFV replication before fusion was affected when the cholesterol trafficking in infected cells was disrupted using a cholesterol transport inhibitor, U18666A. Our data showed that U18666A affected both the fusion and replication steps in the life cycle of the virus, but not its binding and entry steps. The subsequent experiments confirmed that niemann-pick C1 (NPC1), a lysosomal membrane protein that helps cholesterol to leave the lysosome, was affected by U18666A, which led to the accumulation of cholesterol in lysosomes and inhibition of CSFV replication. Imipramine, a cationic hydrophobic amine similar to U18666A, also inhibited CSFV replication via similar mechanism. Surprisingly, the antiviral effect of U18666A was restored by the histone deacetylase inhibitor (HDACi), Vorinostat, which suggested that HDACi reverted the dysfunction of NPC1, and intra-cellular cholesterol accumulation disappeared and CSFV replicability resumed. Together, these data indicated that CSFV transformed from early endosome and late endosome into lysosome after endocytosis for further replication and that U18666A was a potential drug candidate for anti-pestivirus treatment.

1. Introduction

Classical swine fever (CSF) is a highly contagious and fatal disease that causes significant economic losses to the pig industry throughout the world. The CSF virus (CSFV) is a member of the genus *Pestivirus* within the *Flaviviridae* family (Meyers et al., 1996; Paton et al., 2000) and is closely related to other members of the genus, namely, bovine viral diarrhea virus 1 (BVDV-1) (Passler et al., 2014) and BVDV-2 (Kuta et al., 2015), border disease virus (BDV) (Mao et al., 2015; Tautz et al., 2015), an atypical pestivirus isolated from a giraffe (Schirrmeier et al., 2004), and a variety of other unclassified pestiviruses. The CSFV genome consists of a single-stranded, and positive-sense RNA with a single open reading frame (ORF) encoding a polyprotein that is cleaved into 12 mature viral proteins. Of these, the core protein and the envelope glycoproteins E^{rns}, E1, and E2 are structural proteins. E2 is the immunodominant protein in the envelope, and it plays an important role in virus neutralization (Li et al., 2015; Zhou et al., 2011). E2 forms homodimers and heterodimers with glycoprotein E1. The formation of the heterodimer is essential for the entry of pestivirus into cells (Hulst and Moormann, 1997; Wang et al., 2004), therefore, both E1 and E2 are required for virus entry via receptor-mediated endocytosis (Hulst and Moormann, 1997).

Cholesterol is essential for various cellular structures and processes (Cannon et al., 2006; Martin-Acebes et al., 2016). When cholesterol is reduced in host cells, viral production is affected (Desplanques et al., 2010; Medigeshi et al., 2008). Various viruses enter host cells through lipid rafts in which cholesterol is the predominant component (Kim et al., 2017; Verma et al., 2018). The lipid raft is readily disrupted if the membrane cholesterol is selectively extracted by pharmacological agents such as MβCD ((Li et al., 2017a,b; Barman and Nayak, 2007) or Filipin (Wilhelm et al., 2019; Kodam et al., 2010). The membrane cholesterol was shown to be required for virus entry (Geoghegan et al., 2017; Osuna-Ramos et al., 2018; Rosales Ramirez and Ludert, 2019). Our previous studies showed that the membrane cholesterol played a critical role in CSFV internalization (Liu et al., 2017; Shi et al., 2016; Zhang et al., 2018). We then used MβCD to treat the infected cells to confirm that cholesterol affected CSFV egress. However, it remains obscure whether cholesterol in host cells is involved in other steps in

* Corresponding author.
E-mail address: zhoubin@njau.edu.cn (B. Zhou).

https://doi.org/10.1016/j.vetmic.2019.108436
Received 2 July 2019; Received in revised form 9 September 2019; Accepted 1 October 2019

the life cycle of the virus.

U18666A, an intra-cellular cholesterol transport inhibitor, is a widely used chemical to block the intracellular trafficking of cholesterol and to mimic Niemann-Pick type C disease, a hereditary lysosomal storage disease (Amritraj et al., 2013; Koh and Cheung, 2006). The amphipathic property of this compound is believed to be the mechanism of action prompting accumulation of cholesterol in late endosomes and lysosomes (Singhal et al., 2018; Tang et al., 2009). A number of previous studies showed that some viruses were affected by U18666A. The entry and replication of Dengue virus were inhibited by U18666A with the above mentioned mechanism (Poh et al., 2012). Recently, U18666A was found to be capable of inhibiting the replication of Chikungunya virus (CHIKV) in human skin fibroblasts (Wichit et al., 2017). U18666A also blocked the release pathway of mature HCV particles via multivesicular bodies (MVBs) without affecting the viral replication (Elgner et al., 2016).

We have shown that CSFV is transferred from early endosome (Rab5) to late endosome (Rab7) in PK-15 cells after endocytosis (Shi et al., 2016), but no direct evidence has been provided to prove that CSFV are transferred to the proper intracellular sites (lysosome) for membrane fusion and uncoating. This study was to elucidate the antiviral mechanism of U18666A against CSFV replication and the life cycle of CSFV in this process. We used a series of approaches to examine the early step of CSFV post entry into PK-15 cells. The resulting data indicated that loss of function of lysosome caused the inhibition of CSFV transmission, consequently affecting the replication of CSFV.

2. Materials and methods

2.1. Virus and cells

The highly virulent CSFV Shimen strain (GenBank accession number: AF092448) and the highly virulent JEV NJ2008 strain (GenBank accession number: GQ918133) were used in this study. PK-15 or IPEC-J2 cells were cultured at 37 ˚C in the presence of 5% CO_2 in Dulbecco's modified eagle medium (DMEM, Gibco) supplemented with 10% fetal bovine serum (FBS) (Gibco), 0.2% NaHCO3, 100ug/ml streptomycin, and 100 IU/ml penicillin (Gbico).

2.2. Cell infection and drug treatment

U18666A (3β-[2-(diethylamino) ethoxy] an-drost-5-en-17-one) (Sigma-Aldrich, Lot: 2782373), an intracellular cholesterol transport inhibitor, blocks the intracellular trafficking of cholesterol. Imipramine (I0971) was purchased from the TCI Company. Vorinostat (HY-10221) was purchased from MCE. For time of addition experiment of U18666A, cells were pretreated for 16 h with the drug, before virus was added to the cells (16 h pre-treatment) or cells were pretreated for 16 h and the drug remained throughout the 24 h of infection (throughout). Alternatively, the drug was added only during the 1 h of infection when most of the entry and fusion occurred (1 h entry), or after the 1 h of infection (after entry) for the remaining of the infection.

2.3. Cholesterol staining

Cells were stained by Filipin (sc-202511, Santa Cruz) as previously described (Orlandi and Fishman, 1998). Briefly, they were fixed with 4% paraformaldehyde (PFA) for 15 min at room temperature, washed three times with PBS and incubated with Filipin for 30 min at 4 ℃ (Wichit et al., 2017). They were then collected, washed three times with PBS and analyzed by fluorescence microscopy in the DAPI channel.

2.4. Confocal fluorescence microscopy

PK-15 cells grown on dishes were infected with CSFV at MOI of 1 at 4 ℃ for 1 h and and then the temperature was raised to 37 ℃. After incubation, the monolayers were fixed with 4% PFA in PBS and permeabilized with 0.1% Triton X-100. Double-stranded RNA (dsRNA) was labeled by a mouse monoclonal antibody J2 (Scisons). Endoplasmic reticulum (ER) and Golgi apparatus were detected using ER-tracker red (C1041, Beyotime, China), a rabbit anti-GM130 antibody (ab52649), respectively. To visualize Lamp1 and CSFV, cells were stained with a mouse anti-CSFV E2 antibody (WH303) and a rabbit anti-Lamp1 antibody (ab25245). Cholesterol was labeled by Filipin and visualized via the Confocal DAPI channel. The colocalization coefficients were calculated using a professional quantitative co-localization analysis software (Nikon A1; Nikon, Japan) included with a Nikon A1 confocal microscope, and the results were expressed as a Pearson's correlation coefficient (Liu et al., 2017).

2.5. Western blotting

Cells were washed three times with ice-cold PBS and lysed in cold lysis buffer (0.1%Triton X-100 and 1 mM phenylmethylsulfonyl fluoride in PBS) for 30 min. Lysates were clarified by centrifugation at 12,000 ×g for 10 min. Proteins in the lysates were separated by SDS-PAGE, transferred to the nitrocellulose membranes, and then probed with the indicated antibodies. β-actin was used as a loading control. In order to determine proteins levels, the corresponding protein/actin quantity was used to calculate the grayscale using the ImageJ 7.0 software.

2.6. RNAi assay

To knockdown RNA, PK-15 cells were transfected with 100 nM siRNA using Lipofectamine 3000 (Invitrogen) according to the manufacturer's instructions. The siRNA duplexes used in the study were as follows: siNPC1-1 (5′-GCUUACAGCUCAGCCGUUATTUAACGGCUGAG CUGUAAGCTT-3′), siNPC1-2 (5′-GCAUGUUCCUGUCAUCCUUTTAAGG AUGACAGGAACAUGCTT-3′), and siNPC1-3 (5′-GCCCUCGACAAAGUC AGUUTTAACUGACUUUGUCGAGGGCTT-3′). At 24 h–36 h post-transfection, cells were infected with CSFV (MOI of 0.1) and viral RNA was measured by RT-qPCR as described previously.

2.7. Cell viability assay

Cell viability was determined using the MTT-based assay. Briefly, PK-15 cells were treated with different compounds and incubated at 37 ℃, 5% CO_2, washed by phosphate-buffered saline (PBS) and then incubated with 100 μL MTT. 2 h later, MTT was removed and 50 μL of DMSO was added to each well and mixed thoroughly. The mixture was incubated at 37 ℃ for 10 min and cellular viability was determined by measuring the absorbance value at 570 nm.

2.8. Binding and entry assay

Cells were pretreated with subtoxic doses of the drugs at 37 ℃ for 1 h and inoculated with CSFV (MOI of 5) at 4 ℃ for 1 h to allow virus attachment without internalization. Then, the cells were washed with ice-cold PBS three times so that unbound viruses were removed. The culture medium was replaced with fresh serum-free DMEM, and the cells were subsequently shifted to 37 ℃ treatment with 5% CO_2 to allow virus internalization. 1 h later, the cells were washed with citrate buffer solution (pH = 3) to remove the non-internalized virons on the surface of the cells which were then washed three times with ice-cold PBS. Viral RNA was measured by RT-qPCR as described previously.

2.9. Statistical analysis

All data were presented as means ± the standard deviations (SD). A student *t*-test was used to compare the data from the pairs of treated and untreated groups. Statistical significance was indicated by asterisks

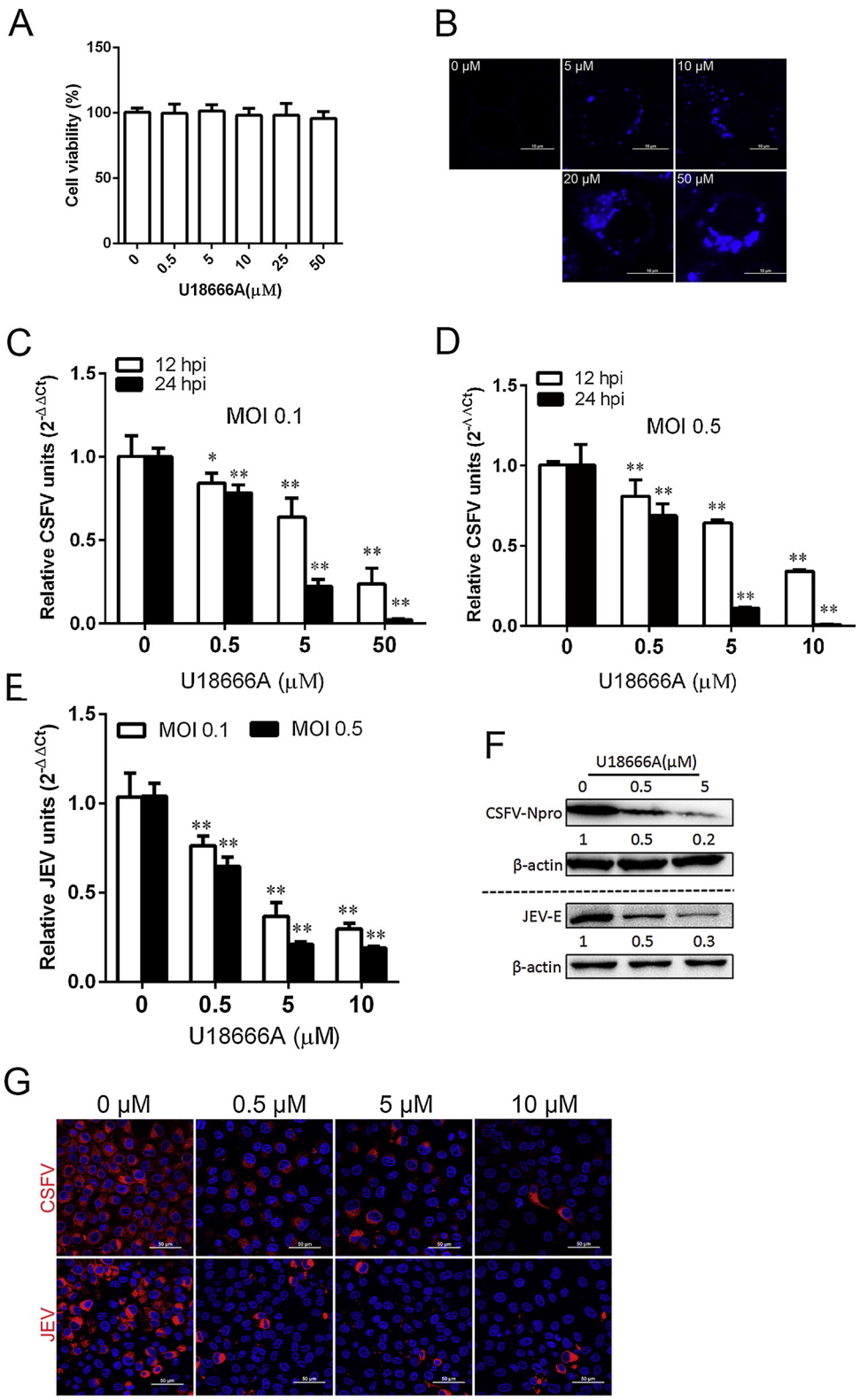

Fig. 1. U18666A causes accumulation of cholesterol and inhibits CSFV replication in PK-15 cells. (A) The effect of U18666A on the cell viability was quantified using an MTT assay kit for cell cytotoxicity. Duplicate experimental data were expressed as means ± the SD. (B) U18666A causes accumulation of cholesterol. PK-15 cells were treated either by DMSO or 0.5, 5, 10 and 50 μM of U18666A for 24 h before fixation and labeling by Filipin (blue). (C and D) PK-15 cells were treated with DMSO or different concentrations of U18666A after infection with CSFV of 0.1 MOI (C) or 0.5 MOI (D) 12 h and 24 h later, viral replication was determined by RT-qPCR. (E) PK-15 cells were treated with DMSO or different concentrations of U18666A after infection with JEV of 0.1 or 0.5 MOI as a control. Later, viral replication was determined by RT-qPCR. (F) The effect of U18666A on CSFV/JEV replication by Western blotting. PK-15 cells were treated with DMSO or different concentrations of U18666A after infection with CSFV/JEV of 0.1 MOI as a control. Later, cells were harvested, lysed and subjected to Western blotting. (G) PK-15 cells were treated with DMSO or different concentrations of U18666A after infection with CSFV or JEV of 0.1 MOI, and viruses were stained in red, and DAPI in blue, and they were visualized by confocal microscopy. All the results were presented as means ± the SD of the data from three independent experiments (*, $P < 0.05$; **, $P < 0.01$). (For interpretation of the references to colour in this figure legend, the reader is referred to the web version of this article).

(*, $P < 0.05$; **, $P < 0.01$) in the figures. All statistical analyses and calculations were performed using Prism 6 (GraphPad Software, Inc, La Jolla, CA).

3. Results

3.1. U18666A inhibits CSFV replication

Cholesterol has been shown to play an important role in viral infection of permissive cells. In order to see whether CSFV replication was affected due to the accumulation of intracellular cholesterol, PK-15 cells were pretreated with U18666A for 12 h before infection with the

CSFV Shimen strain. U18666A did not have any cytotoxic effects within 36 h, even at the highest concentration of 50 μM (Fig. 1A). Treatment of cells with increasing concentrations of U18666A resulted in a dose-dependent accumulation of intracellular cholesterol in the LE/Ls (late endosome and lysosomes) compartment (Fig. 1B). Pretreatment of the cells for 12 h with U18666A to allow the accumulation of cholesterol, prior to infection by CSFV for 12 and 24 h, resulted in a dose-dependent inhibition of viral replication. The effect of the drug was more prominent at the 24 h time point (hpi), as shown by a decrease in the number of viral RNA copies in the infected cells incubated with MOI 0.1 or 0.5, being close to 100% at the highest concentration of 10 μM (Fig. 1C and D). Interestingly, U18666A also strongly inhibited the replication of the other Flaviviridae family member, Japanese encephalitis virus (JEV). The similar antiviral phenotype showed that the number of viral RNA copies and protein levels were reduced significantly in a dose-dependent manner (Fig. 1E and F). Finally, confocal microscopy after 24 h post infection showed that both CSFV and JEV replications with the red fluorescence signals were reduced significantly in a dose-dependent manner (Fig. 1G). Coherently, U18666A inhibited CSFV replication.

3.2. U18666A does not affect CSFV binding and entry

To investigate whether the early steps of the CSFV life cycle were affected by U18666A, the effect on the binding of CSFV to and its entry into the target cells in the presence or absence of U18666A was analyzed. Pretreatment of the PK-15 cells with U18666A did not lead to a decrease in CSFV binding and entry (Fig. 2A). However, as a control, this compound inhibited JEV entry but not binding in a dose-dependent manner (Fig. 2B), which was consistent with a previous report (Poh et al., 2012).

In order to further understand the inhibitory effect of U18666A in cells, we operated the time of addition experiment. U18666A (5 μM) was added to PK-15 cells before and during infection. When the cells were pretreated for 12 h to allow accumulation of cholesterol in late endosome/lysosome, a slight decline of virus infection was observed (Fig. 2C, 12 h pretreatment). However, we did not observe dramatic reduction of virus production when U18666A was given to the cells for only 1 h during the virus entry (Fig. 2C, 1 h entry), likely because the treatment was not sufficiently long to allow the accumulation of cholesterol in the endocytic pathway. Furthermore, we observed obvious reduction of virus infection when U18666A was added 1 h after virus infection and stayed present for the rest of the infection period of 24 h. This suggested that U18666A might have an impact in the later stages of virus infection, possibly on membrane fusion or uncoating. When we combined both the pretreatments and left the U18666A compound alone throughout the infection period, a far greater magnitude of viral reduction was observed. JEV, as a control virus, was found to be a more obvious inhibitor. With U18666A inhibiting JEV entry, the results showed that any treatment of this compound might cause a significant decrease in the number of JEV RNA copies (Fig. 2D). We also found that the number of viral RNA copies significantly reduced along with the treatment of IPEC-J2 cells with U18666A (Fig. 2E), which was consistent with result shown in Fig. 2C. Overall, U18666A had a post entry inhibiton of CSFV.

3.3. U18666A affects CSFV replication post entry

We continued to explore at which step U18666A influenced the viral replication. First, we performed the function of U18666A on accumulation of cholesterol in lysosome which was observed in the punctated intracellular organelles by Filipin staining. Filipin labeling in treated cells co-localized with the lysosome marker Lamp1 as expected, showing the accumulation of cholesterol in the lysosome compartment (Fig. 3A). The Pearson's overlap coefficient of cholesterol and Lamp1 was calculated in the DMSO- and U18666A-treated cells (Fig. 3B). Western blot confirmed that the protein level of Lamp1 increased gradually along with the increasing concentrations of U18666A (Fig. 3C). Second, we checked the location of viral particles in the cells after U18666A treatment. As shown in Fig. 3D, in the DMSO-treated cells, virus particles were observed in the punctated structures in the cytoplasm at 1 h post infection (1 hpi). In the DMSO-treated cells, E2 proteins were no longer detected at 4 h and 8 h post infections, presumably because of the fusion of the viral particles and the release of the capsid into the cytoplasm (4 hpi and 8 hpi). Newly synthesized viral E2 proteins re-appeared at the time-point of 12 hpi, localizing in the peri-nuclear regions of the infected cells (12 hpi). However, in the drug-treated cells where the cholesterol transport was arrested by U18666A, many viral particles could be observed at 4 and 8 hpi (U18666A 4 h and 8 h) and much less staining of the newly synthesized E2 protein was seen at 12 h and 24 h post infections (U18666A 12 h and 24 h). Confocal microscopy showed that CSFV replication was inhibited due to the blocking of the cholesterol trafficking by U18666A in the lysosome. At 4 and 8 hpi, viral trafficking was hampered in these cholesterol-loaded endosomes and accumulation of cholesterol in the late endosome/lysosome was inhibitory in CSFV trafficking. Under the condition where the endo-lysosome compartment was loaded with an extra amount of cholesterol, we speculated that it was possible that CSFV no longer carried out proper fusion or subsequent uncoating. Consequently, a reduced level of viral genome released into the cytoplasm caused much less virus production at 12 and 24 hpi. Finally, cells were treated with U18666A at 1 hpi and they still contained U18666A for 3 h, and were fixed for confocal microscopy. As shown in Fig. 3E, virions and Lamp1 showed significant colocalization in U18666A or the Imipramine treated cells, while less was observed with virions and Lamp1 in the DMSO treated cells. The colocalization coefficients were expressed as the Pearson's correlation coefficient, measured for individual cells. Fig. 3F showed that the Pearson's correlation coefficient of U18666A or Imipramine was more significant than that of DMSO after CSFV endocytosis. We concluded that U18666A affected CSFV replication post entry.

3.4. NPC1 protein is crucial for CSFV replication

Nieman-Pick type C disease, a hereditary neurovisceral disorder, impairs egress of cholesterol from the LE/Ls compartment resulting in intracellular cholesterol accumulation in the lysosome (Newton et al., 2018; Pfeffer, 2019). As U18666A and imipramine mimicked an NPC-deficient phenotype (Wichit et al., 2017), we followed an alternative approach to study the consequence of intracellular cholesterol accumulation on CSFV replication, using siRNA to knockdown NPC1 protein. First, the protein levels of NPC1 did not obviously change along with the increasing concentrations of U18666A (Fig. 4A), suggesting that U18666A did not affect NPC1 transcription and translation. Second, we used commercial siRNA to study the effect of NPC1 on CSFV replication. In Fig. 4B and C, RT-qPCR and Western blot showed that the number of NPC1 mRNA copies or the protein levels of the siNPC1-1, -2 or -3 treated cells were decreased, compared with that of the siCtrl-treated cells. As was expected, the siNPC1-1, -2 or -3 treated cells showed an intracellular accumulation of cholesterol, revealed by staining with Filipin (Fig. 4D). Moreover, Filipin staining colocalized with that of Lamp1 (a large amount of co-localization), indicating that cholesterol accumulated specifically in the LE/Ls compartment of these siRNA-treated cells (Fig. 4D). However, the protein levels of Lamp1 of the siNPC1-1, -2 or -3 treated cells were clearly up-regulated, compared with that of the siCtrl-treated cells (Fig. 4E), which was consistent with the results shown in Fig. 3B. Absence of the NPC1 protein resulted in a strong decrease in CSFV infection, as shown by RT-qPCR and confocal microscopy (Fig. 4F and G). These results showed that NPC1 deficiency had a strong impact on the life cycle of CSFV.

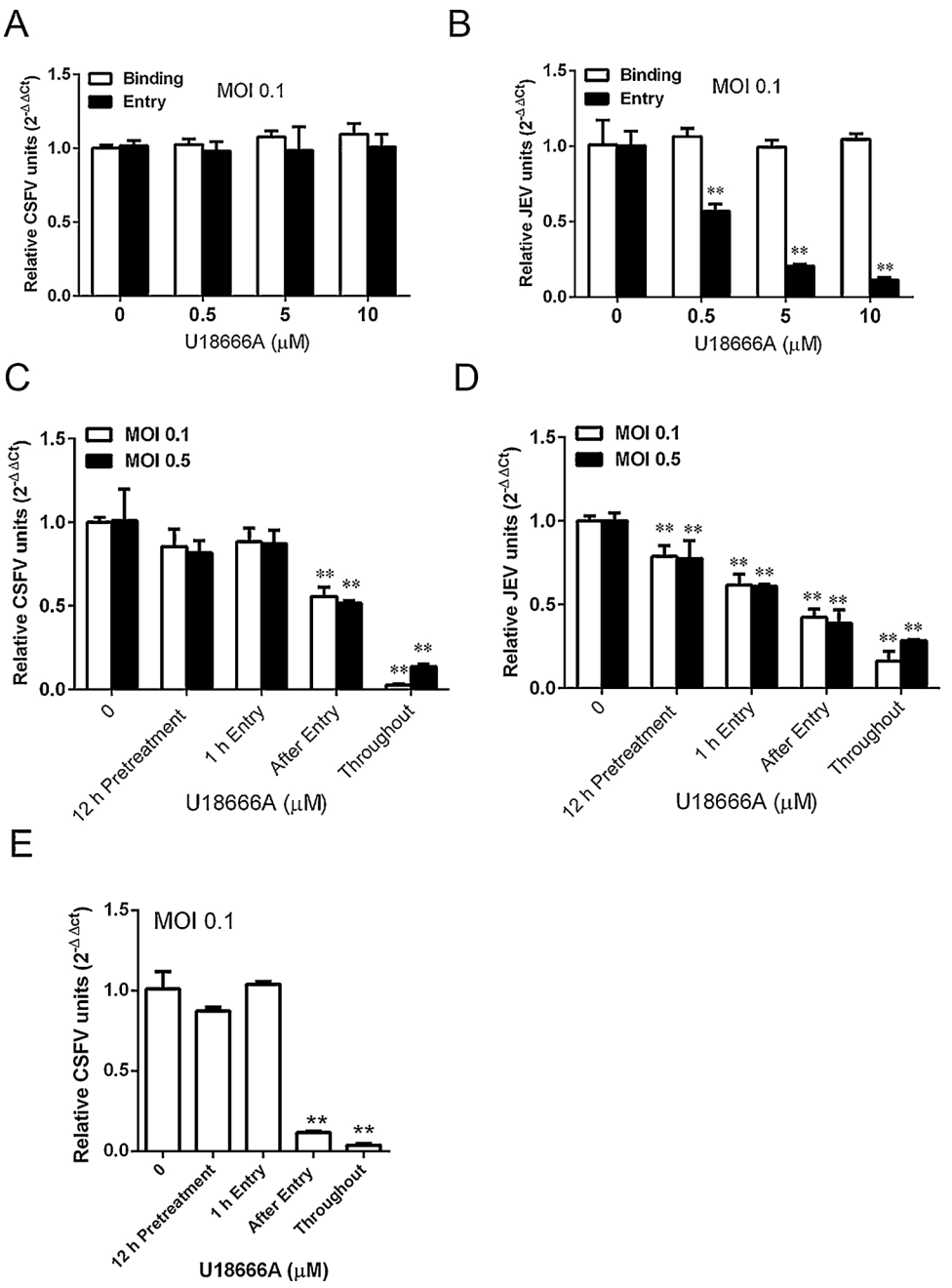

Fig. 2. U18666A does not affect CSFV binding and entry. (A and B) Different concentrations of U18666A were used to inoculate PK-15 cells for 2 h, CSFV/JEV at MOI of 5 for 1 h at 4 °C, and then at 37 °C at 0 hpi (binding) or 1 hpi (entry). Bound virus was removed by short trypsin treatment before analysis of entered virus by RT-qPCR. (C and D) Time point of addition of U18666A in CSFV or JEV infection. PK-15 cells were treated with U18666A (5 μM) at various time-points during the infection by CSFV or JEV of MOI 0.1. Viral replication was determined by RT-qPCR.(i) "12 h Pretreatment" meant that PK-15 cells were pretreated with U18666A for 12 h ; (ii) "1 h Entry" menat that PK-15 cells were treated with U18666A and CSFV for 1 h. After that, the mixture was washed and treated with 2% DMEM; (iii) "After Entry" meant that PK-15 cells were treated with U18666A 1 h after CSFV entry; (iv) "Throughout" menat that PK-15 cells were treated with U18666A for the whole time period including 12 h pretreatment. (E) After CSFV of MOI 0.1 infection, viral replication was determined by RT-qPCR along with the treatment of IPEC-J2 cells with U18666A, which agreed with that of the PK-15 cells. All the results were presented as means ± the SD of the data from three independent experiments (*, $P < 0.05$; **, $P < 0.01$).

3.5. Imipramine also exerts antiviral activity against CSFV

U18666A inhibits CSFV replication by causing cholesterol accumulation in lysosomes. In order to confirm the antiviral effects, we extended the study by using another alike compound, imipramine Imipramine which is a cationic hydrophobic amine and can induce lysosomal accumulation of numerous lipid species, including cholesterol. Like U18666A, imipramine strongly inhibited the replication of CSFV in the PK-15 cells in a dose-dependent manner. This result showed that the number of viral RNA copies was dramatically decreased when CSFV of either 0.1 or 0.5 MOI was incubated in the drug-treated cells as described previously. RNA replication was effectively inhibited up to 100% at a concentration of 25 or 50 μM (Fig. 5B), without any deleterious effect on cell viability (Fig. 5A). Fig. 5C showed that imipramine significantly inhibited CSFV replication despite different kinds of treatment, indicating that this alternative compound impaired both the entry and replication of CSFV. Confocal microscopy showed that the red fluorescence signals expressing virus replication significantly reduced with the increasing concentration of imipramine (Fig. 5D), which was consistent with the data from RT-qPCR. Treatment of cells with increasing concentrations of imipramine resulted in a dose-dependent accumulation of intracellular cholesterol in the lysosome (Fig. 5E), which was consistent with the function of U18666A. Finally, Western blot confirmed that the treatment of imipramine caused a dose-dependent accumulation of Lamp1 (Fig. 5F), but the protein level of NPC1 did not vary in the presence of the increasing concentration of imipramine (Fig. 5G), suggesting that there was a similar molecular mechanism upon imipramine.

3.6. HDACi reverses the inhibitory effect of U18666A

The histone deacetylase inhibitor (HDACi) has been reported to revert the U18666A-induced dysfunction of NPC1. We assumed that inhibition of CSFV replication by U18666A was associated with the loss

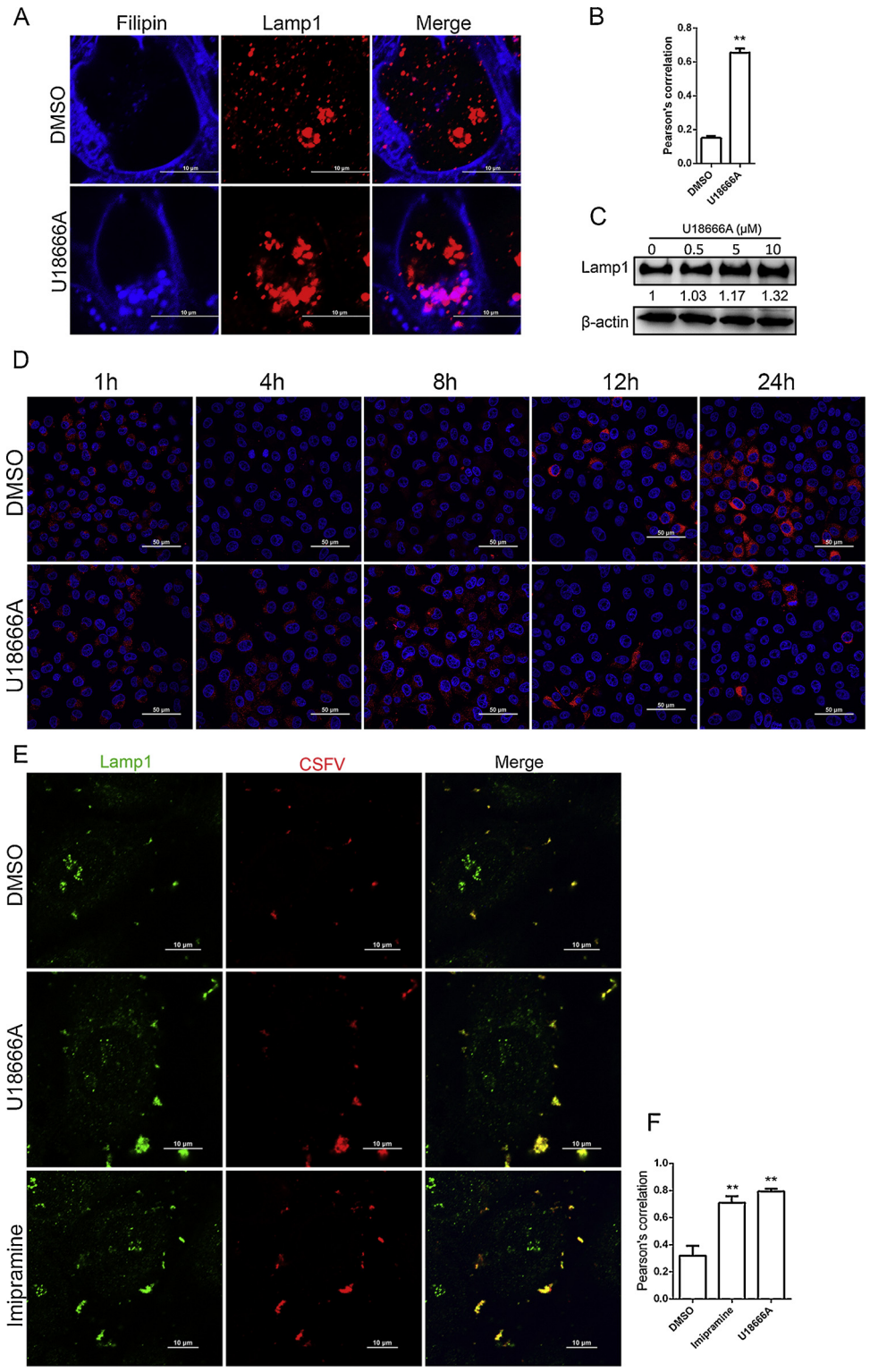

Fig. 3. The effect of U18666A on virus trafficking in cells. (A) U18666A causes accumulation of cholesterol in the lysosome. PK-15 cells were treated by DMSO or 5 μM of U18666A for 24 h before fixation and labeling by Filipin (blue) or Lamp1 (Red). The fluorescence intensity of Lamp1 was measured in DMSO- and U18666A-treated cells. (B) Pearson's overlap coefficient of cholesterol and Lamp1 was calculated in the DMSO- and U18666A-treated cells. (C) Western blotting determined accumulation of cholesterol in the lysosome. PK-15 cells were treated by DMSO or different concentrations of U18666A for 24 h. Later, cells were harvested, lysed and subjected to Western blotting by using the anti-Lamp1 antibody. (D) For viral trafficking study: DMSO- and U18666A-treated cells were infected with CSFV at various time-points of infection (1, 4, 8, 12 and 24 h), and cells were fixed and stained with the anti-E2 antibody (WH303) (red). (E) PK-15 cells were infected with CSFV of MOI 5 for 1 h, and maintained with U18666A (5 μM) or Imipramine as a drug control for 3 h before fixation and labelling by Lamp1 (Green) or CSFV (Red). (F) Pearson's overlap coefficient of virions and Lamp1 was calculated in the DMSO-, Imipramine- or U18666A-treated cells. All the results were presented as means ± the SD of the data from three independent experiments (*, $P < 0.05$; **, $P < 0.01$). (For interpretation of the references to colour in this figure legend, the reader is referred to the web version of this article).

of NPC1 function. We further examined whether HDACi, which restores NPC1 function, could resolve U18666A-induced cholesterol accumulation and inhibition of viral replication. When an HDACi, Vorinostat, was added to the U18666A-pretreated cells, cholesterol accumulation was reduced (Fig. 6A). The influence of Vorinostat on CSFV replication was investigated using confocal microscopy and RT-qPCR. The viral E2 protein levels specifically decreased in the infected cells pretreated with U18666A. On the other hand, the addition of Vorinostat to the U18666A-pretreated cells increased the level of the viral E2 protein. Addition of Vorinostat to the culture in the presence of U18666A restored CSFV replication (Fig. 6B). RT-qPCR showed that the number of viral RNA copies did not change with the addition of Vorinostat to the U18666A-pretreated cells (Fig. 6C), compared with that of the untreated control. Overall, HDACi reversed the inhibitory effect of U18666A on CSFV replication.

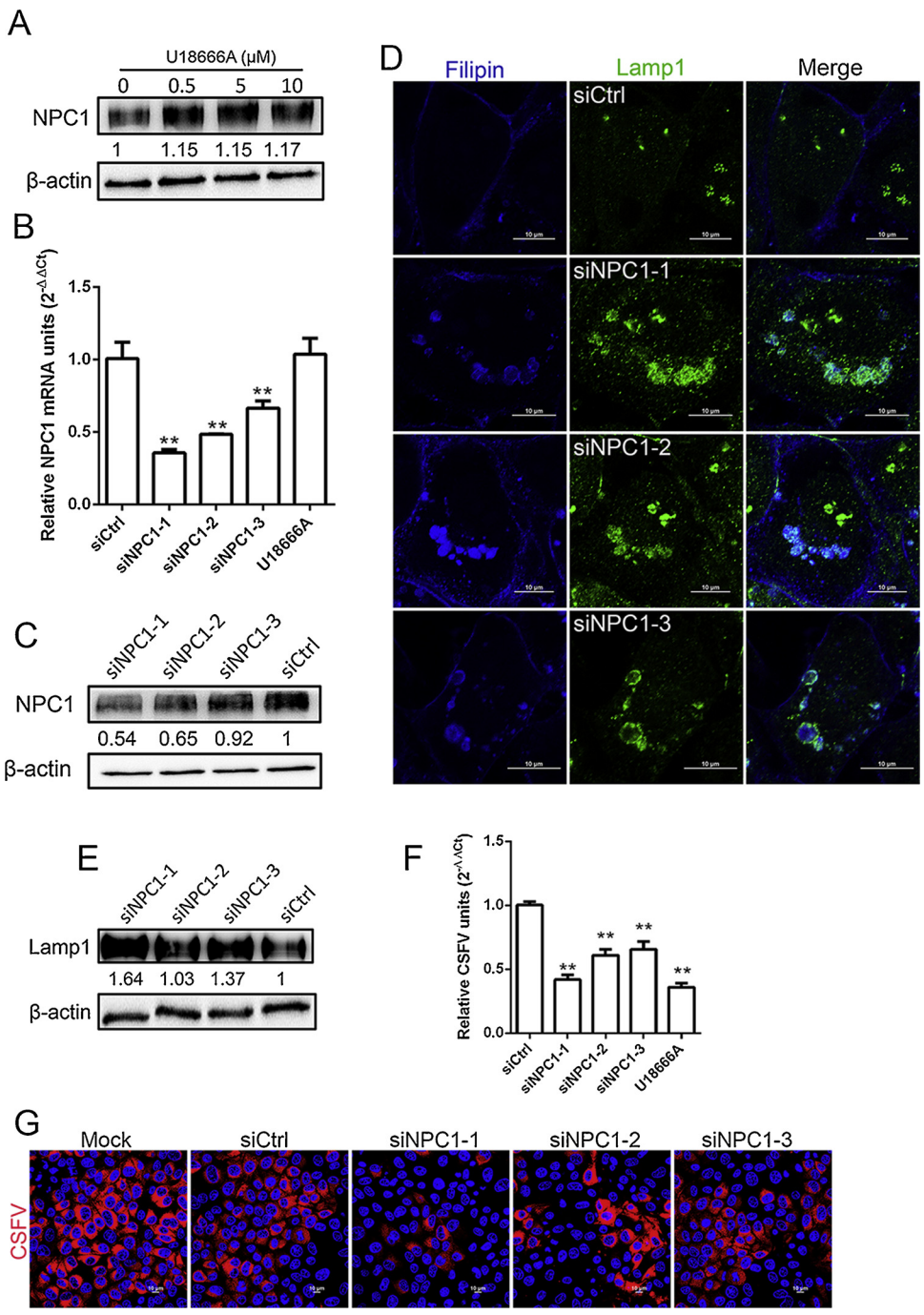

Fig. 4. NPC1 protein is crucial for CSFV replication. (A) NPC1 protein levels do not dramatically change in the presence of U18666A. PK-15 cells were cultivated with U18666A (5 μM) for 24 h. Cells were lysed and protein was extracted. Western blotting was performed to determine the relative levels of the NPC1 protein. (B and C) Knockdown of NPC1 protein. PK-15 cells were treated with siRNAs targeting NPC1 or a control siRNA for 24 h. The mRNA or protein level of NPC1 was assessed using RT-qPCR or Western blotting. (D) Knockdown of NPC1 causes accumulation of cholesterol in the lysosome. Cells were transfected with either siCtrl, siNPC1-1, -2 or -3 for 48 h, and were then fixed and labeled by Filipin (blue) or Lamp1 (green). Scale bar, 10 μm. (E) Western blotting was used to determine the knockdown efficiency of siLamp-1. The siCtrl, siNPC1-1,-2 or -3 transfected cells were harvested, lysed and transferred to nitrocellulose membranes, and were then probed with the indicated antibodies. β-actin was used as a loading control. In order to determine the levels of Lamp1 proteins, the corresponding protein/actin quantity was used to calculate the grayscale using the ImageJ 7.0 software. (F) PK-15 cells were transfected with siNPC1-1, -2 or -3 for 48 h before infection with CSFV (MOI = 0.5). 24 h later, virus RNA was measured by RT-qPCR. The quantification was based on three independent experiments. The results were presented as means ± the SD of the data from three independent experiments (**, $P < 0.01$). (G) PK-15 cells were transfected with siCtrl, siNPC1-1, -2 or -3 for 48 h before infection with CSFV (MOI = 0.5). 24 h later, cells were fixed and labeled using the anti-E2 antibody (WH303). Scale bar, 10 μm. (For interpretation of the references to colour in this figure legend, the reader is referred to the web version of this article).

4. Discussion

Cholesterol has been shown to play an important role in viral infection of permissive cells. U18666A is a cationic amphiphilic drug (CAD) impairing cholesterol biosynthesis and intracellular transport (Cenedella et al., 2005; Cenedella, 2009). It also inhibits cholesterol release from lysosomes by impairing the function of a cholesterol transporter, Niemann-Pick type C1 (NPC1) (Ko et al., 2001). As has been described, U18666A can directly bind to a site that is within a section of the NPC1 protein called the sterol-sensing domain. This binding blocks the movement of cholesterol out of lysosomes.

It has been reported that U18666A suppresses replication of Ebola virus, dengue virus, and human hepatitis C virus (Elgner et al., 2016; Lu et al., 2015; Poh et al., 2012). However, no studies have demonstrated the relationship between U18666A and CSFV replication. In the present study, we found that U18666A blocked the movement of cholesterol out of lysosomes and inhibited CSFV infection. It dramatically inhibited viral replication, but such inhibition had no relationship with the viral binding or entry. We used JEV as a control virus, and interestingly, found that U18666A inhibited the entry and replication but not the binding step of JEV infection. This was consistent with the previous research on DENV, an important member of the same genus (Poh et al., 2012). We speculated that the molecular effect of U18666A on JEV inhibition might be similar to that on DENV inhibition. CSF remains one of the most economically important viral diseases of domestic pigs and wild boar worldwide (Brown and Bevins, 2018; Rossi et al., 2015). It is not sufficient to eradicate CSF by vaccination alone, and the development of supplemental antiviral strategies is necessary (Li et al., 2017a,b; Luo et al., 2014). Some anti-CSFV drugs, such as Imidazo[4,5-*c*]pyridines (Vrancken et al., 2009, 2008), and uridine derivatives of 2-

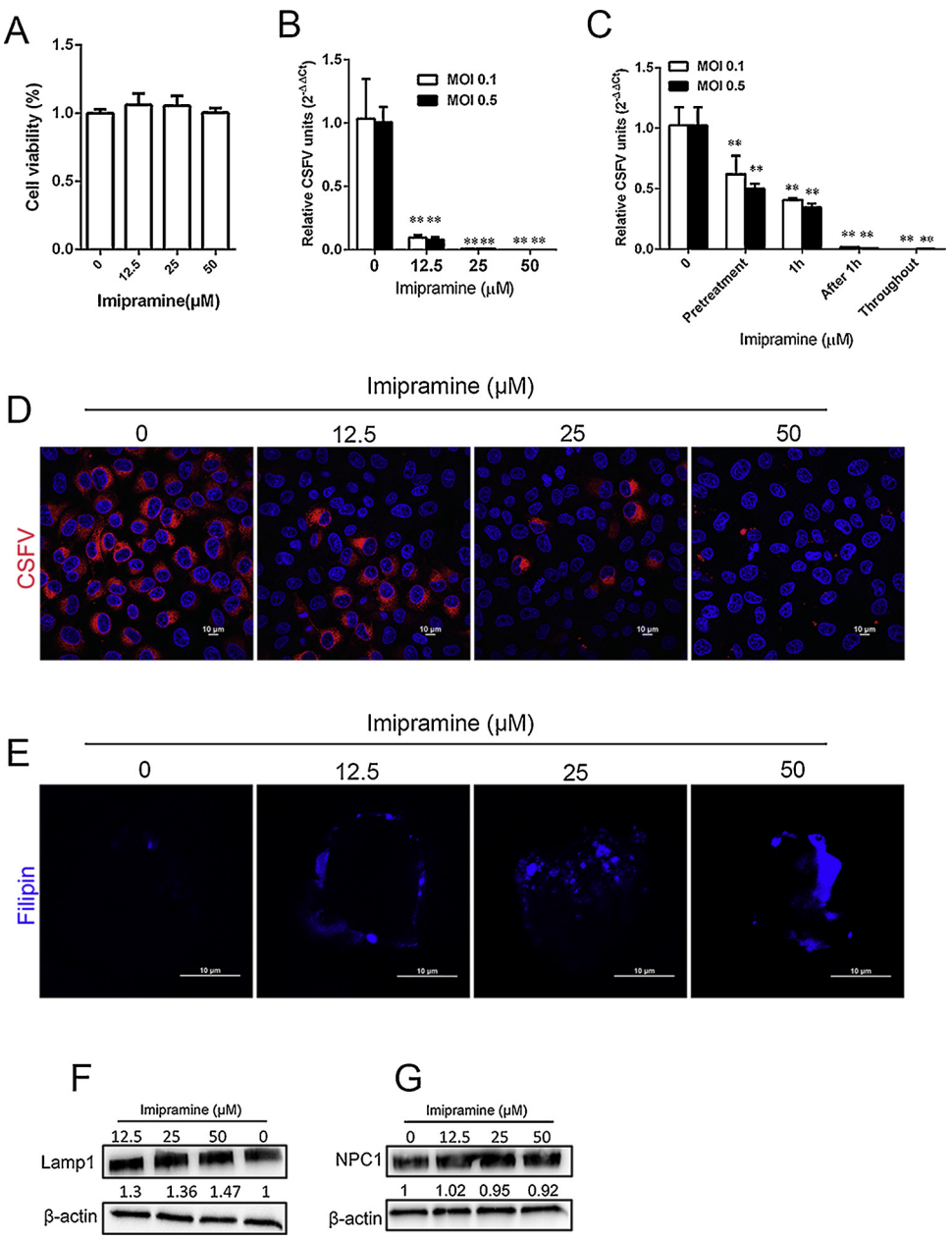

Fig. 5. Imipramine also exerts antiviral activity against CSFV. (A)The effect of Imipramine on the cell viability was quantified using an MTT assay kit for cell cytotoxicity. Duplicated experimental data were expressed as means ± the SD. (B) PK-15 cells were treated with DMSO or different concentrations of Imipramine after infection with CSFV of MOI 0.1 or 0.5. 24 h later, viral RNA was determined by RT-qPCR. The results were presented as means ± the SD of the data from three independent experiments (**, $P < 0.01$). (C) PK-15 cells were treated with Imipramine at 25 μM at various time-points in the course of infection. viral RNA was determined by RT-qPCR. The results were presented as means ± the SD of the data from three independent experiments (**, $P < 0.01$). (D) PK-15 cells were treated with DMSO or different concentrations of Imipramine after infection with CSFV. Viruses were stained in red using the anti-E2 antibody (WH303) and visualized by confocal microscopy. Scale bar, 10 μm. (E) PK-15 cells were treated either by DMSO or 6.25, 12.5, 25 and 50 μM of Imipramine for 24 h before fixation and labeling by Filipin. Scale bar, 10 μm. (F and G) Western blotting was used to determine the role of Imipramine. PK-15 cells were treated either by DMSO or 12.5, 25 and 50 μM of Imipramine for 24 h. Cells were harvested, lysed and transferred to nitrocellulose membranes, and were then probed with the indicated antibodies. β-actin was used as a loading control. In order to determine the levels of Lamp1 and NPC1 proteins, the corresponding protein/actin quantity was used to calculate the grayscale using the ImageJ 7.0 software. (For interpretation of the references to colour in this figure legend, the reader is referred to the web version of this article).

deoxy sugars (Krol et al., 2013), have been reported. The early steps of the life cycle of the virus, its binding to and entry into the host cells, are crucial determinants of infection and are potential targets for the development of antiviral therapies. Therefore, U18666A is a potential antiviral drug against CSFV, but their clinical effect and practical application for CSF control require further investigation and development.

Our previous work demonstrated that Rab5, Rab7 and Lamp1 were involved in CSFV infection and that knockdown of Lamp1 caused a reduction in CSFV infection (Zhang et al., 2018), implying the endolysosomal pathway was involved in CSFV endocytosis. We assumed that CSFV particles were firstly transferred to early endosomes in a Rab5-dependent manner, that a Rab7-dependent pathway guided CSFV to late endosomes, and that a Rab11-dependent pathway later guided CSFV to recycling endosomes. Finally, CSFV was transferred into lysosomes (Lamp1) where membrane fusion occurred and then viral RNA was released. Treatment of U18666A contributed to cholesterol accumulation in lysosomes. The present result showed that CSFV accumulated in lysosome within 4 h after entering the cell, but did not go on to the next step of membrane fusion.In Fig. 3E, we could see that viral particles co-located with lysosome, including another similar drug, imipramine. In the untreated cells, we could scarcely see the co-localization of the virus. Virus replication went on successfully, and at 24 h after infection, the virus was obviously duplicated. Previous research showed that the endolysosomal pathway was composed of at least three distinct populations of vesicles: Rab7-, Lamp1-, and Rab7/Lamp1 vesicles (Ng et al., 2012). The majority of endolysosomal vesicles were positive for both Rab7 and Lamp1. Therefore, we observed the co-localization of Rab7 and Lamp1 under the treatment of the drug, indicating that the transmission of the virus was inhibited at the endolysosomal stage (data not shown). When the endolysosomal compartment was loaded with an extra amount of cholesterol, we speculated that that CSFV might no longer carry out proper fusion or subsequent uncoating. At 12 and 24 hpi, the protein level of CSFV E2 in the U18666A-treated cells decreased obviously, compared with that in the control, indicating a decrease in virus production. Therefore, we hypothesized that less release of viral genome led to a decrease in viral production at 12 and 24 hpi (Fig. 3D). Furthermore, confocal microscopy showed that viral RNA decreased significantly in the presence of

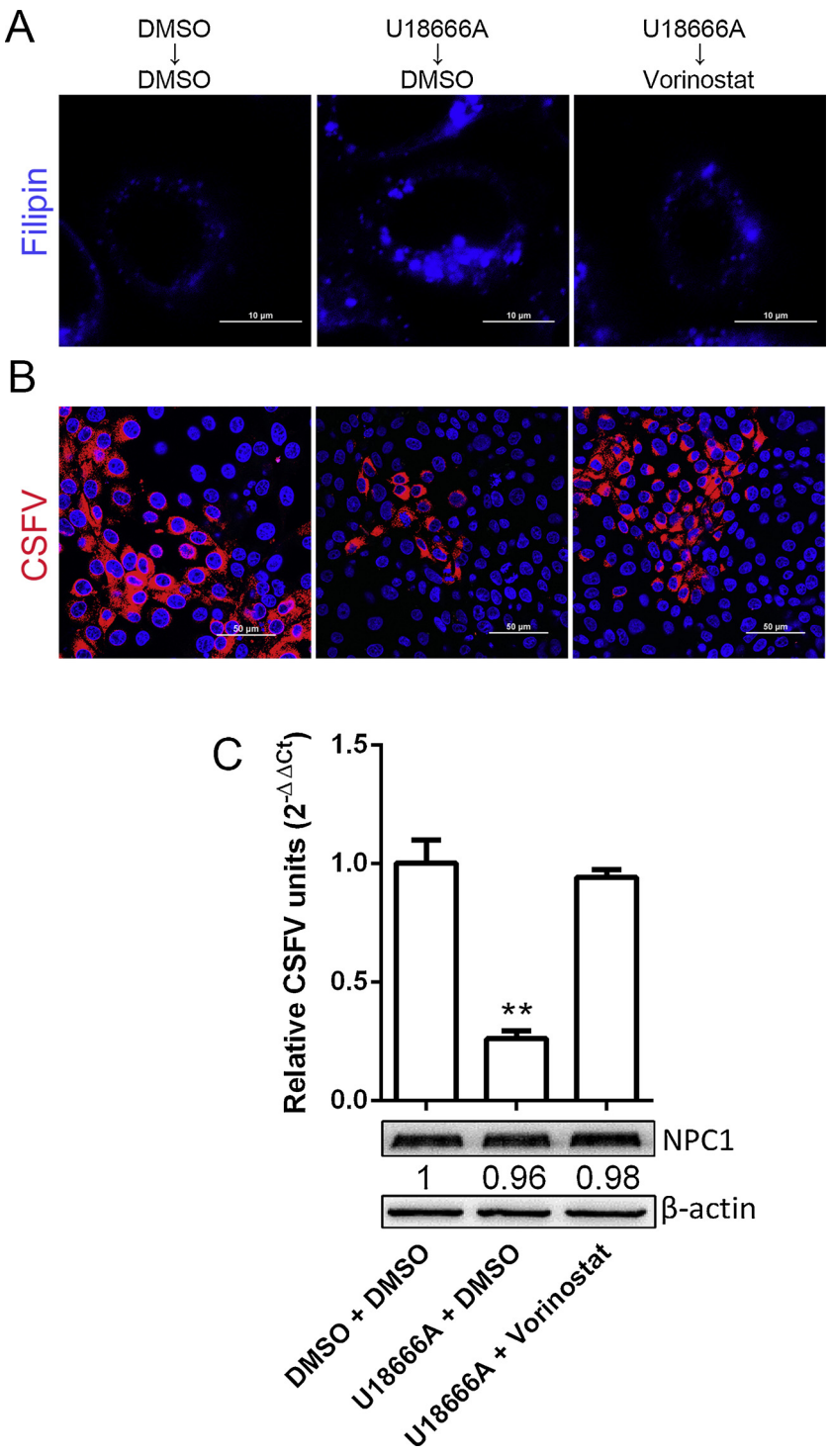

Fig. 6. Vorinostat reverts the U18666A-induced antiviral activity by cholesterol accumulation. (A) Vorinostat reverts cholesterol accumulation. Cells were treated with U18666A (5 μM) or DMSO for 12 h and then with Vorinostat or DMSO for 12 h. Cells were fixed and labeled by Filipin in blue. Scale bar, 10 μm. (B) Vorinostat reverts CSFV infection. The treated cells, described above, were fixed and stained using the anti-E2 antibody (WH303). Scale bar, 50 μm. (C) Vorinostat reverts the effect of U18666A on CSFV replication. The treated cells, described above, were harvested and lysed; and then viral RNA was determined by RT-qPCR. Alternatively, the lysed cells were subjected to Western blotting using the indicated antibodies. The results were presented as means ± the SD of the data from three independent experiments (**, $P < 0.01$). (For interpretation of the references to colour in this figure legend, the reader is referred to the web version of this article).

U18666A (Fig. S1). The present data confirmed our hypothesis that CSFV was transmitted to lysosomes after entering the cells for the next step of replication. In addition, Fig. S1 showed U18666A treatment had no effect on the distribution of Endoplasmic reticulum (ER) and Golgi apparatus, suggesting that the drugs didn't target later stages of the CSFV life cycle.

U18666A is an inhibitor of the cholesterol transporter NPC1 (Ko et al., 2001). It binds NPC1 and suppresses its function (Lu et al., 2015). In this study, Imipramine, which hinders the functionof NPC1 function in a similarly manner to that of U18666A, also inhibited CSFV replication. To verify this this function of Imipramine, we first investigated the effect of the NPC1 protein on CSFV replication. We knocked down NPC1, which led to the accumulation of cholesterol and Lamp1. This was a mutual proof that NPC1 was necessary for virus replication. We speculated that the loss of NPC1 function was the real mechanism of viral replication inhibition. In contrast to U18666A, HDACi reverts the dysfunction of NPC1 (Banerjee et al., 2018; Pipalia et al., 2017). It has been reported that HDACi treatment enhances the expression of some protein chaperonins or directly modulates the activity of chaperones by altering their acetylation status, which corrects the storage defect in some NPC1 deficiency cell lines (Pipalia et al., 2017). Therefore, we believed that HDACi restored the activity of NPC1 in the presence of U18666A in this study. When Vorinostat was added to the U18666A-treated cells, intracellular cholesterol accumulation

disappeared and CSFV replication resumed. To our knowledge, reversion of U18666A-induced inhibition of viral replication of the family of Flaviviridae by HDACi has not previously been reported. It is necessary to determine whether the same phenomenon can be observed in the Zika virus, the dengue virus and HCV.

In conclusion, our results demonstrated that the capability of U18666A to inhibit CSFV replication by interrupting cholesterol trafficking. Essentially, the treatment with drugs resulted in the loss of the function of the cholesterol transfer protein (NPC1), followed by a decline in viral infection, which implied the importance of NPC1 protein in viral replication. Follow-up research is necessary for better understanding of the underlying mechanism of NPC1. However, the present study proved the therapeutic potential of such drugs in CSF treatment.

Acknowledgements

This work was supported by grant from the State Key Laboratory of Veterinary Etiological Biology, Lanzhou Veterinary Research Institute, Chinese Academy of Agricultural Sciences (SKLVEB2017KFKT003), and by National Natural Science Foundation of China (31872471and31572554). We thank Dr. Zhengchun Lv of Cornell University for critical reading and editing of the manuscript.

Appendix A. Supplementary data

Supplementary material related to this article can be found, in the online version, at doi:https://doi.org/10.1016/j.vetmic.2019.108436.

References

Amritraj, A., Wang, Y., Revett, T.J., Vergote, D., Westaway, D., Kar, S., 2013. Role of cathepsin D in U18666A-induced neuronal cell death: potential implication in Niemann-Pick type C disease pathogenesis. J. Biol. Chem. 288, 3136–3152. https://doi.org/10.1074/jbc.M112.412460.

Banerjee, N.S., Moore, D.W., Broker, T.R., Chow, L.T., 2018. Vorinostat, a pan-HDAC inhibitor, abrogates productive HPV-18 DNA amplification. Proc. Natl. Acad. Sci. U. S. A. 115, E11138–E11147. https://doi.org/10.1073/pnas.1801156115.

Barman, S., Nayak, D.P., 2007. Lipid raft disruption by cholesterol depletion enhances influenza A virus budding from MDCK cells. J. Virol. 81, 12169–12178. https://doi.org/10.1128/JVI.00835-07.

Brown, V.R., Bevins, S.N., 2018. A review of classical swine fever virus and routes of introduction into the United States and the potential for virus establishment. Front. Vet. Sci. 5, 31. https://doi.org/10.3389/fvets.2018.00031.

Cannon, B., Lewis, A., Metze, J., Thiagarajan, V., Vaughn, M.W., Somerharju, P., Virtanen, J., Huang, J., Cheng, K.H., 2006. Cholesterol supports headgroup superlattice domain formation in fluid phospholipid/cholesterol bilayers. J. Phys. Chem. B 110, 6339–6350. https://doi.org/10.1021/jp0558371.

Cenedella, R.J., 2009. Cholesterol synthesis inhibitor U18666A and the role of sterol metabolism and trafficking in numerous pathophysiological processes. Lipids 44, 477–487. https://doi.org/10.1007/s11745-009-3305-7.

Cenedella, R.J., Sexton, P.S., Krishnan, K., Covey, D.F., 2005. Comparison of effects of U18666A and enantiomeric U18666A on sterol synthesis and induction of apoptosis. Lipids 40, 635–640. https://doi.org/10.1007/s11745-005-1426-9.

Desplanques, A.S., Pontes, M., De Corte, N., Verheyen, N., Nauwynck, H.J., Vercauteren, D., Favoreel, H.W., 2010. Cholesterol depletion affects infectivity and stability of pseudorabies virus. Virus Res. 152, 180–183. https://doi.org/10.1016/j.virusres.2010.06.008.

Elgner, F., Ren, H., Medvedev, R., Ploen, D., Himmelsbach, K., Boller, K., Hildt, E., 2016. The intracellular cholesterol transport inhibitor U18666A inhibits the exosome-dependent release of mature hepatitis C virus. J. Virol. 90, 11181–11196. https://doi.org/10.1128/JVI.01053-16.

Geoghegan, V., Stainton, K., Rainey, S.M., Ant, T.H., Dowle, A.A., Larson, T., Hester, S., Charles, P.D., Thomas, B., Sinkins, S.P., 2017. Perturbed cholesterol and vesicular trafficking associated with dengue blocking in Wolbachia-infected Aedes aegypti cells. Nat. Commun. 8, 526. https://doi.org/10.1038/s41467-017-00610-8.

Hulst, M.M., Moormann, R.J., 1997. Inhibition of pestivirus infection in cell culture by envelope proteins E(rns) and E2 of classical swine fever virus: E(rns) and E2 interact with different receptors. J. Gen. Virol. 78 (Pt 11), 2779–2787. https://doi.org/10.1099/0022-1317-78-11-2779.

Kim, J.Y., Wang, L., Lee, J., Ou, J.J., 2017. Hepatitis C virus induces the localization of lipid rafts to autophagosomes for its RNA replication. J. Virol. 91. https://doi.org/10.1128/JVI.00541-17.

Ko, D.C., Gordon, M.D., Jin, J.Y., Scott, M.P., 2001. Dynamic movements of organelles containing Niemann-Pick C1 protein: NPC1 involvement in late endocytic events. Mol. Biol. Cell 12, 601–614. https://doi.org/10.1091/mbc.12.3.601.

Kodam, A., Maulik, M., Peake, K., Amritraj, A., Vetrivel, K.S., Thinakaran, G., Vance, J.E., Kar, S., 2010. Altered levels and distribution of amyloid precursor protein and its processing enzymes in Niemann-Pick type C1-deficient mouse brains. Glia 58, 1267–1281. https://doi.org/10.1002/glia.21001.

Koh, C.H., Cheung, N.S., 2006. Cellular mechanism of U18666A-mediated apoptosis in cultured murine cortical neurons: bridging Niemann-Pick disease type C and Alzheimer's disease. Cell. Signal. 18, 1844–1853. https://doi.org/10.1016/j.cellsig.2006.04.006.

Krol, E., Wandzik, I., Gromadzka, B., Nidzworski, D., Rychlowska, M., Matlacz, M., Tyborowska, J., Szewczyk, B., 2013. Anti-influenza A virus activity of uridine derivatives of 2-deoxy sugars. Antiviral Res. 100, 90–97. https://doi.org/10.1016/j.antiviral.2013.07.014.

Kuta, A., Wozniakowski, G., Polak, M.P., 2015. Cross-priming amplification for detection of bovine viral diarrhoea virus species 1 and 2. J. Appl. Microbiol. 119, 632–639. https://doi.org/10.1111/jam.12859.

Li, L., Yu, L., Hou, X., 2017a. Cholesterol-rich lipid rafts play a critical role in bovine parainfluenza virus type 3 (BPIV3) infection. Res. Vet. Sci. 114, 341–347. https://doi.org/10.1016/j.rvsc.2017.04.009.

Li, S., Wang, J., Yang, Q., Naveed Anwar, M., Yu, S., Qiu, H.J., 2017b. Complex virus-host interactions involved in the regulation of classical swine fever virus replication: a minireview. Viruses 9. https://doi.org/10.3390/v9070171.

Li, W., Mao, L., Zhou, B., Liu, X., Yang, L., Zhang, W., Jiang, J., 2015. The swine CD81 enhances E2-based DNA vaccination against classical swine fever. Vaccine 33, 3542–3548. https://doi.org/10.1016/j.vaccine.2015.05.055.

Liu, C.C., Zhang, Y.N., Li, Z.Y., Hou, J.X., Zhou, J., Kan, L., Zhou, B., Chen, P.Y., 2017. Rab5 and Rab11 are required for clathrin-dependent endocytosis of Japanese encephalitis virus in BHK-21 cells. J. Virol. 91. https://doi.org/10.1128/JVI.01113-17.

Lu, F., Liang, Q., Abi-Mosleh, L., Das, A., De Brabander, J.K., Goldstein, J.L., Brown, M.S., 2015. Identification of NPC1 as the target of U18666A, an inhibitor of lysosomal cholesterol export and Ebola infection. eLife 4. https://doi.org/10.7554/eLife.12177.

Luo, Y., Li, S., Sun, Y., Qiu, H.J., 2014. Classical swine fever in China: a minireview. Vet. Microbiol. 172, 1–6. https://doi.org/10.1016/j.vetmic.2014.04.004.

Mao, L., Liu, X., Li, W., Yang, L., Zhang, W., Jiang, J., 2015. Characterization of one sheep border disease virus in China. Virol. J. 12, 15. https://doi.org/10.1186/s12985-014-0217-9.

Martin-Acebes, M.A., Vazquez-Calvo, A., Saiz, J.C., 2016. Lipids and flaviviruses, present and future perspectives for the control of dengue, Zika, and West Nile viruses. Prog. Lipid Res. 64, 123–137. https://doi.org/10.1016/j.plipres.2016.09.005.

Medigeshi, G.R., Hirsch, A.J., Streblow, D.N., Nikolich-Zugich, J., Nelson, J.A., 2008. West Nile virus entry requires cholesterol-rich membrane microdomains and is independent of alphavbeta3 integrin. J. Virol. 82, 5212–5219. https://doi.org/10.1128/JVI.00008-08.

Meyers, G., Thiel, H.J., Rumenapf, T., 1996. Classical swine fever virus: recovery of infectious viruses from cDNA constructs and generation of recombinant cytopathogenic defective interfering particles. J. Virol. 70, 1588–1595. https://jvi.asm.org/content/70/3/1588/article-info.

Newton, J., Milstien, S., Spiegel, S., 2018. Niemann-pick type C disease: the atypical sphingolipidosis. Adv. Biol. Regul. 70, 82–88. https://doi.org/10.1016/j.jbior.2018.08.001.

Ng, E.L., Gan, B.Q., Ng, F., Tang, B.L., 2012. Rab GTPases regulating receptor trafficking at the late endosome-lysosome membranes. Cell Biochem. Funct. 30, 515–523. https://doi.org/10.1002/cbf.2827.

Osuna-Ramos, J.F., Reyes-Ruiz, J.M., Del Angel, R.M., 2018. The role of host cholesterol during flavivirus infection. Front. Cell. Infect. Microbiol. 8, 388. https://doi.org/10.3389/fcimb.2018.00388.

Orlandi, P.A., Fishman, P.H., 1998. Filipin-dependent inhibition of cholera toxin: evidence for toxin internalization and activation through caveolae-like domains. J. Cell Biol. 141, 905–915. https://doi.org/10.1083/jcb.141.4.905.

Passler, T., Riddell, K.P., Edmondson, M.A., Chamorro, M.F., Neill, J.D., Brodersen, B.W., Walz, H.L., Galik, P.K., Zhang, Y., Walz, P.H., 2014. Experimental infection of pregnant goats with bovine viral diarrhea virus (BVDV) 1 or 2. Vet. Res. 45, 38. https://doi.org/10.1186/1297-9716-45-38.

Paton, D.J., McGoldrick, A., Greiser-Wilke, I., Parchariyanon, S., Song, J.Y., Liou, P.P., Stadejek, T., Lowings, J.P., Bjorklund, H., Belak, S., 2000. Genetic typing of classical swine fever virus. Vet. Microbiol. 73, 137–157. https://doi.org/10.1016/S0378-1135(00)00141-3.

Pfeffer, S.R., 2019. NPC intracellular cholesterol transporter 1 (NPC1)-mediated cholesterol export from lysosomes. J. Biol. Chem. 294, 1706–1709. https://doi.org/10.1074/jbc.TM118.004165.

Pipalia, N.H., Subramanian, K., Mao, S., Ralph, H., Hutt, D.M., Scott, S.M., Balch, W.E., Maxfield, F.R., 2017. Histone deacetylase inhibitors correct the cholesterol storage defect in most Niemann-Pick C1 mutant cells. J. Lipid Res. 58, 695–708. https://doi.org/10.1194/jlr.M072140.

Poh, M.K., Shui, G., Xie, X., Shi, P.Y., Wenk, M.R., Gu, F., 2012. U18666A, an intracellular cholesterol transport inhibitor, inhibits dengue virus entry and replication. Antiviral Res. 93, 191–198. https://doi.org/10.1016/j.antiviral.2011.11.014.

Rosales Ramirez, R., Ludert, J.E., 2019. The dengue virus nonstructural protein 1 (NS1) is secreted from mosquito cells in association with the intracellular cholesterol transporter chaperone caveolin complex. J. Virol. 93. https://doi.org/10.1128/JVI.01985-18.

Rossi, S., Staubach, C., Blome, S., Guberti, V., Thulke, H.H., Vos, A., Koenen, F., Le Potier, M.F., 2015. Controlling of CSFV in European wild boar using oral vaccination: a review. Front. Microbiol. 6, 1141. https://doi.org/10.3389/fmicb.2015.01141.

Schirrmeier, H., Strebelow, G., Depner, K., Hoffmann, B., Beer, M., 2004. Genetic and antigenic characterization of an atypical pestivirus isolate, a putative member of a novel pestivirus species. J. Gen. Virol. 85, 3647–3652. https://doi.org/10.1099/vir.0.80238-0.

Shi, B.J., Liu, C.C., Zhou, J., Wang, S.Q., Gao, Z.C., Zhang, X.M., Zhou, B., Chen, P.Y., 2016. Entry of classical swine fever virus into PK-15 cells via a pH-, dynamin-, and cholesterol-dependent, clathrin-mediated endocytic pathway that requires Rab5 and Rab7. J. Virol. 90, 9194–9208. https://doi.org/10.1128/JVI.00688-16.

Singhal, A., Szente, L., Hildreth, J.E.K., Song, B., 2018. Hydroxypropyl-beta and -gamma cyclodextrins rescue cholesterol accumulation in Niemann-Pick C1 mutant cell via lysosome-associated membrane protein 1. Cell Death Dis. 9, 1019. https://doi.org/10.1038/s41419-018-1056-1.

Tang, Y., Leao, I.C., Coleman, E.M., Broughton, R.S., Hildreth, J.E., 2009. Deficiency of niemann-pick type C-1 protein impairs release of human immunodeficiency virus type 1 and results in Gag accumulation in late endosomal/lysosomal compartments. J. Virol. 83, 7982–7995. https://doi.org/10.1128/JVI.00259-09.

Tautz, N., Tews, B.A., Meyers, G., 2015. The molecular biology of Pestiviruses. Adv. Virus Res. 93, 47–160. https://doi.org/10.1016/bs.aivir.2015.03.002.

Verma, D.K., Gupta, D., Lal, S.K., 2018. Host lipid rafts play a major role in binding and endocytosis of influenza a virus. Viruses 10. https://doi.org/10.3390/v10110650.

Vrancken, R., Haegeman, A., Dewulf, J., Paeshuyse, J., Puerstinger, G., Tignon, M., Le Potier, M.F., Neyts, J., Koenen, F., 2009. The reduction of CSFV transmission to untreated pigs by the pestivirus inhibitor BPIP: a proof of concept. Vet. Microbiol. 139, 365–368. https://doi.org/10.1016/j.vetmic.2009.06.026.

Vrancken, R., Paeshuyse, J., Haegeman, A., Puerstinger, G., Froeyen, M., Herdewijn, P., Kerkhofs, P., Neyts, J., Koenen, F., 2008. Imidazo[4,5-c]pyridines inhibit the in vitro replication of the classical swine fever virus and target the viral polymerase. Antiviral Res. 77, 114–119. https://doi.org/10.1016/j.antiviral.2007.09.006.

Wang, Z., Nie, Y., Wang, P., Ding, M., Deng, H., 2004. Characterization of classical swine fever virus entry by using pseudotyped viruses: E1 and E2 are sufficient to mediate viral entry. Virology 330, 332–341. https://doi.org/10.1016/j.virol.2004.09.023.

Wichit, S., Hamel, R., Bernard, E., Talignani, L., Diop, F., Ferraris, P., Liegeois, F., Ekchariyawat, P., Luplertlop, N., Surasombatpattana, P., Thomas, F., Merits, A., Choumet, V., Roques, P., Yssel, H., Briant, L., Misse, D., 2017. Imipramine inhibits chikungunya virus replication in human skin fibroblasts through interference with intracellular cholesterol trafficking. Sci. Rep. 7, 3145. https://doi.org/10.1038/s41598-017-03316-5.

Wilhelm, L.P., Voilquin, L., Kobayashi, T., Tomasetto, C., Alpy, F., 2019. Intracellular and plasma membrane cholesterol labeling and quantification using filipin and GFP-D4. Methods Mol. Biol. 1949, 137–152. https://doi.org/10.1007/978-1-4939-9136-5_11.

Zhang, Y.N., Liu, Y.Y., Xiao, F.C., Liu, C.C., Liang, X.D., Chen, J., Zhou, J., Baloch, A.S., Kan, L., Zhou, B., Qiu, H.J., 2018. Rab5, Rab7, and Rab11 are required for caveola-dependent endocytosis of classical swine fever virus in porcine alveolar macrophages. J. Virol. 92. https://doi.org/10.1128/JVI.00797-18.

Zhou, B., Liu, K., Jiang, Y., Wei, J.C., Chen, P.Y., 2011. Multiple linear B-cell epitopes of classical swine fever virus glycoprotein E2 expressed in E. coli as multiple epitope vaccine induces a protective immune response. Virol. J. 8, 378. https://doi.org/10.1186/1743-422X-8-378.